The American Journal of Pathology, Vol. 171, No. 2, August 2007

DOI: 10.2353/ajpath.2007.070188

Cell Injury, Repair, Aging and Apoptosis

Linking of Autophagy to Ubiquitin-Proteasome System Is Important for the Regulation of Endoplasmic Reticulum Stress and Cell Viability

Wen-Xing Ding,* Hong-Min Ni,* Wentao Gao,* Tamotsu Yoshimori,† Donna B. Stolz,‡ David Ron,§ and Xiao-Ming Yin*

From the Departments of Pathology and Cell Biology and Physiology,‡ University of Pittsburgh School of Medicine, Pittsburgh, Pennsylvania; the Department of Cell Genetics,† National Institute of Genetics, Mishima, Japan; and the Skirball Institute of Biomolecular Medicine,§ New York University School of Medicine, New York, New York*

Two major protein degradation systems exist in cells, the ubiquitin proteasome system and the autophagy machinery. Here, we investigated the functional relationship of the two systems and the underlying mechanisms. Proteasome inhibition activated autophagy, suggesting that the two are functionally coupled. Autophagy played a compensatory role as suppression of autophagy promoted the accumulation of polyubiquitinated protein aggregates. Autophagy was likely activated in response to endoplasmic reticulum stress caused by misfolded proteins during proteasome inhibition. Suppression of a major unfolded protein response pathway mediated by IRE1 by either gene deletion or RNA interference dramatically suppressed the activation of autophagy by proteasome inhibitors. Interestingly, c-Jun NH_2-terminal kinase (JNK) but not XBP-1, both of which are the known downstream targets of IRE1, seemed to participate in autophagy induction by proteasome inhibitors. Finally, proteasome inhibitor-induced autophagy was important for controlling endoplasmic reticulum stress and reducing cell death in cancer cells. Our studies thus provide a mechanistic view and elucidate the functional significance of the link between the two protein degradation systems. ***(Am J Pathol 2007, 171:513–524; DOI: 10.2353/ajpath.2007.070188)***

The ubiquitin-proteasome system (UPS) is a major degradation system for short-lived proteins.[1] Proteins to be degraded are labeled with ubiquitin. The ubiquitinated proteins are degraded by the 26S proteasome complex. The degradation is thus specifically targeted to a fraction of proteins. Prompt removal of these proteins is critical to the precise and timely regulation of intracellular signaling involved in multiple cellular processes, including cell proliferation and cell death.

UPS is also important for the degradation of misfolded proteins exporting from the endoplasmic reticulum (ER). It is the degrading machine in the ER-associated degradation pathway.[2] Endoplasmic reticulum is an intracellular membranous structure that performs such important functions as protein post-translational modifications, protein folding and oligomerization, and synthesis of lipids and sterols. Proteins may fail to be properly modified or folded due to mutations or ER dysfunction. The abnormal proteins would be exported to the cytosol to be degraded mainly by the proteasomes (ER-associated degradation). Suppression of UPS can thus lead to the build-up of the misfolded proteins in the ER, leading to significant ER stress.

ER stress could be induced by many other stimuli in ER, such as the changes in calcium homeostasis, redox status, or glycosylation.[3] The unfolded protein response (UPR) is the major protective and compensatory mechanism during ER stress.[3,4] The UPR promotes protein folding via the up-regulated ER protein chaperones and the degradation of misfolded proteins via the up-regulation of the ER-associated degradation components.[3,4] However, if the stress is too severe or lasts for too long, decompensation of ER function could induce cell death.[5]

Macroautophagy (referred as autophagy hereafter) is another major intracellular degradation system. Unlike the UPS, autophagy is mainly responsible for the degradation of long-lived proteins and other cellular contents.[6,7] It is a bulk degradation system, usually activated

Supported in part by National Institutes of Health funds (grants CA83817, CA111456, and NS45252 to X.-M.Y.). Work in D.R.'s laboratory was supported by National Institute of Health grants DK47119 and ES0861. W.-X.D. is a recipient of the American Liver Foundation/Alpha-1 Foundation scholar award.

Accepted for publication May 4, 2007.

Address reprint requests to Xiao-Ming Yin, M.D., Ph.D., Department of Pathology, University of Pittsburgh School of Medicine, Scaife Hall, Room S739, 3550 Terrace St., Pittsburgh, PA 15231. E-mail: xmyin@pitt.edu.

in response to adverse environment, such as the deprivation of nutrients or growth factors.[8] Autophagy also plays a role in development,[6] in defending against microbial infections,[9] and in the pathogenesis of a number of diseases including cancer.[10] At least 27 *Atg* genes have been defined to participate in autophagy or autophagy-related process.[11] The functions of Atg8/LC3B, Atg7, Atg6/Beclin 1, and Atg5 are among the best characterized in the mammalian cells. Although the proteins targeted by autophagy and the UPS are different, the two systems serve a similar purpose in degrading proteins and recycling amino acids. However, the functional connection between the two systems and how they could be inter-regulated is not well understood.

In the current study, we demonstrate that the two cellular degradation systems are functionally coupled and suppression of UPS activates autophagy. Autophagy is activated by proteasome inhibitor-induced ER stress via the IRE1-mediated pathway. In this context, autophagy functions to purge polyubiquitinated protein aggregates induced by proteasome inhibitors and alleviate ER stress. Consequently, autophagy can protect cells from the toxicity of proteasome inhibitors. These findings thus may provide useful insight into the understanding of the pathogenesis of diseases involving proteasome inhibition and misfolded proteins, such as neurodegenerative diseases, and also in the design of effective cancer therapy where proteasome inhibitors are used.

Materials and Methods

Reagents

The following antibodies were used: anti-Atg6/Beclin 1 (BD Biosciences, San Jose, CA), anti-Atg8/LC3B,[12] anti-Atg5,[13] anti-BiP (Sigma, St. Louis, MO), anti-ATF4 (Santa Cruz Biotechnology, Santa Cruz, CA), anti-CHOP (Santa Cruz Biotechnology), anti-calnexin (Santa Cruz Biotechnology), anti-β-actin (Sigma), anti-ubiquitin (Santa Cruz Biotechnology), and horseradish peroxidase-labeled secondary antibodies (Jackson ImmunoResearch Laboratories, West Grove, PA). SP600125 (catalog no. 420119) is a specific JNK inhibitors obtained from Calbiochem (San Diego, CA). All other chemicals were from Sigma or Invitrogen (Carlsbad, CA).

Plasmids, siRNA, and Transfection

One to 2 μg of GFP-LC3B was transfected into 2×10^5 cells using Effectene according to the supplier's protocol (Qiagen, Valencia, CA). Stable cell lines expressing GFP-LC3B were constructed using a retroviral vector and selected using neomycin. Small interfering RNAs (siRNAs) (0.24 μmol/L) were transfected into 1×10^6 cells using Oligofectamine (Invitrogen) for 48 hours before analysis. siRNAs (Invitrogen) against the following human genes were used: *Atg5* (5′-GGACGAAUUCCAACUUGUU-3′), *Atg6/Beclin1* (5′-GGUCUAAGACGUCCAACAA-3′), *Atg7* (5′-GCCAGUGGGUUUGGAUCAA-3′), and *Atg8*/LC3B (5′-GAAGGCGCUUACAGCUCAA-3′).

Cell Culture and Microscopy

HCT 116 Bax-positive and Bax-deficient cell lines[14] were maintained in McCoy's 5A with the routine supplements. DU145 and PC3 cell lines were maintained in Dulbecco's modified Eagle's medium or F12K with routine supplements. Phase and fluorescence images were acquired under a fluorescence microscope (Nikon Eclipse TE200; Melville, NY) using the SPOT RT Slider digital camera and the companion software (Diagnostics Instruments, Sterling Heights, MI). The signals were pseudo-colored using the same software. Confocal microscopy was performed for some samples using an Olympus Fluoview 1000 inverted microscope and the companion software (Olympus, Tokyo, Japan). Changes in the intracellular GFP-LC3B pattern were observed in live cells. To quantify the change, the average number of GFP-LC3B puncta per cell was determined from a randomly selected pool of 50 to 60 cells under each condition.

For the examination of acidic compartments, cells cultured on coverslips were first treated as indicated in the Figure 2 legend and then stained with monodansylcadaverine (MDC) for 5 minutes before being fixed with 4% paraformaldehyde and observed using the green fluorescence filter. For the immunostaining assay, cells were immunostained with the anti-ubiquitin or anti-calnexin antibody followed by Cy3-conjugated secondary antibody as previously described.[15]

For electron microscopy, cells were fixed with 2% paraformaldehyde and 2% glutaraldehyde in 0.1 mol/L phosphate buffer (pH 7.4), followed by 1% OsO_4. After dehydration, thin sections were stained with uranyl acetate and lead citrate for observation under a JEM 1011CX electron microscope (JEOL, Peabody, MA). Images were acquired digitally. The average number of autophagic vacuoles (AVs) per field of 100 μm^2 of the cytoplasm was determined from a randomly selected pool of 10 to 15 fields under each condition.

Analysis of Cell Death

Apoptotic cells with condensed or fragmented nuclei were analyzed with Hoechst 33342 (5 μg/ml) staining. All images were obtained using digital fluorescence microscopy as described above. Analysis of caspase activity was performed as previously described.[15]

Immunoblot Assay

Cells were washed in phosphate-buffered saline and lysed in radioimmunoprecipitation assay buffer. Forty micrograms of protein was separated by sodium dodecyl sulfate-polyacrylamide gel electrophoresis and transferred to polyvinylidene difluoride polyvinylidene difluoride membranes. The membranes were stained with the indicated primary and secondary antibodies and developed with SuperSignal West Pico chemiluminescent substrate (Pierce, Rockford, IL).

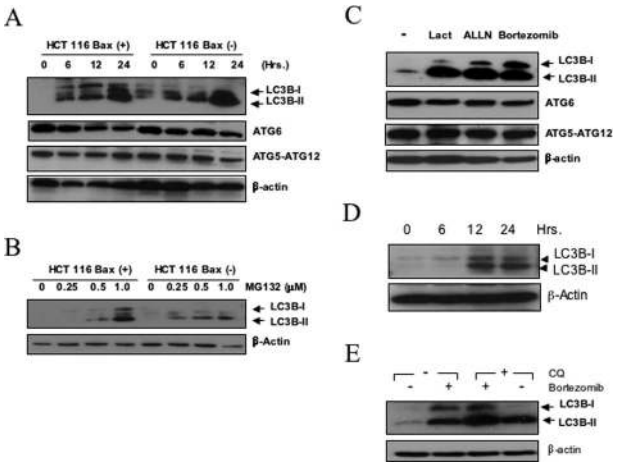

Figure 1. Proteasome inhibition leads to accumulation of LC3B-II. **A** and **B:** Bax-positive and -deficient HCT 116 cells were treated with MG132 (1 μM) for different times (**A**) or at different doses for 16 hours (**B**). Total lysates were prepared and subjected to immunoblot analysis. Atg5 was detected as the complex with Atg12.[51] **C:** Bax-deficient HCT 116 cells were treated with lactacystin (5 μmol/L), ALLN (10 μmol/L), or bortezomib (20 nmol/L) for 24 hours, and immunoblot analysis was conducted as above. **D:** DU145 cells were treated with MG132 (5 μmol/L) for different times and immunoblot analysis was conducted as above. **E:** Bax-deficient HCT 116 cells were treated with bortezomib (20 nmol/L) in the presence or absence of chloroquine (CQ, 2 μmol/L) for 24 hours. Immunoblot assay was then conducted as indicated.

Statistical Analysis

Experimental data were subjected to Z-test or one way analysis of variance analysis with Scheffé's post hoc test where appropriate.

Results

Inhibition of Proteasome Induced Autophagy

The two protein degradation systems seem to be functionally coupled as inhibition of proteasome rapidly activated autophagy. MG132, a commonly used proteasome inhibitor, could elicit a time-dependent and dose-dependent accumulation of LC3B-II, a lipidated form of LC3B, which is localized on the autophagic vacuoles (AVs),[12] in the colon cancer cell line HCT116, regardless of the presence of a proapoptosis molecule, Bax (Figure 1, A and B). Other proteasome inhibitors, including bortezomib, which is currently used in clinic for refractory multiple myeloma, were also able to induce LC3B-II accumulation (Figure 1C). In addition, this phenomenon could be observed in other types of cells, including the prostate cancer cell line DU145 (Figure 1D) and murine embryonic fibroblasts (MEFs) (see below). Disruption of lysosome function with chloroquine led to further increases in LC3B-II, suggesting that there was indeed a net increase of LC3B-II following proteasome inhibition (Figure 1E). On the other hand, the expression levels of other major Atg molecules, such as Atg5, Atg6/Beclin 1, and Atg7 did not seem to change significantly (Figure 1, A and C; data not shown).

Consistent with these findings, cells transfected with a GFP-LC3B construct exhibited a transition of the GFP-LC3B signals from the diffusive cytoplasmic pattern to the punctated membrane pattern following treatment with proteasome inhibitors (Figure 2, A–C), suggesting the localization of LC3B-II to the AVs. Inhibition of proteasome function also induced a significant increase of cells with punctated MDC staining (Figure 2, D and E), suggesting an overall increase in the acidic cellular compartments, mainly the lysosomes and the autophagolysosomes.[9,16] Correspondingly, some of the GFP-LC3B puncta were well correlated with the MDC puncta (Figure 2D).

Most convincingly, electron microscopic examination of MG132-treated cells indicated a considerable increase of AVs at various stages (Figure 3, A and B). Autophagic vacuoles of both double and multiple membranes could be found as described previously in other scenarios.[17] In addition, early autophagosomes sequestering cytosol, mitochondrion, or endoplasmic reticulum membranes could be readily observed. The occurrence of AVs could be effectively suppressed by 3-methyadenine (3-MA), a known autophagy inhibitor.[18] 3-MA also inhibited the formation of LC3B-II induced by MG132 (Figure 3C). These data collectively argue strongly for the induction of macroautophagy by the inhibition of proteasome function in several types of cells.

Proteasome Inhibitor-Induced Autophagy Constituted a Protection Mechanism against Cell Death in Tumor Cells

We then investigated how autophagy might affect proteasome inhibitor-induced cell death. Proteasome inhibitor-induced apoptosis in HCT 116 cells was preferentially mediated by the pro-death Bcl-2 family protein Bax, and thus the Bax-deficient HCT 116 cells were quite resistant to MG132-induced apoptosis (Figure 4A). Interestingly, inhibition of autophagy by 3-MA enhanced the apoptotic cell death induced by MG132 in not only Bax-positive HCT 116 cells but also in Bax-negative HCT 116 cells (Figure 4A). To confirm the finding, we suppressed the expression of *Atg5*, *Atg6/Beclin1*, *Atg7*, or *Atg8/LC3B* using specific siRNA molecules in the Bax-deficient HCT 116 cells as well as DU145 cells (Figure 4B). Such treatments in general effectively suppressed MG132-induced formation of LC3B-II and autophagic vacuoles (Figure 4C; data not shown). Apoptotic cell death was consistently significantly enhanced in the siRNA-treated cells with elevated caspase activation following the treatment with MG132 (Figure 4, D and E) or other proteasome inhibitors (data not shown). These observations indicate that autophagy played a prosurvival role on proteasome inhibition in these cells, and suppressing autophagy increased the sensitivity of cells to apoptotic stimulation even in the absence of Bax.

Suppression of Autophagy Enhanced Proteasome Inhibitor-Induced Accumulation of Polyubiquitinated Proteins and Endoplasmic Reticulum Stress

Based on these findings, we reasoned that autophagy might act at an upstream point that would regulate the

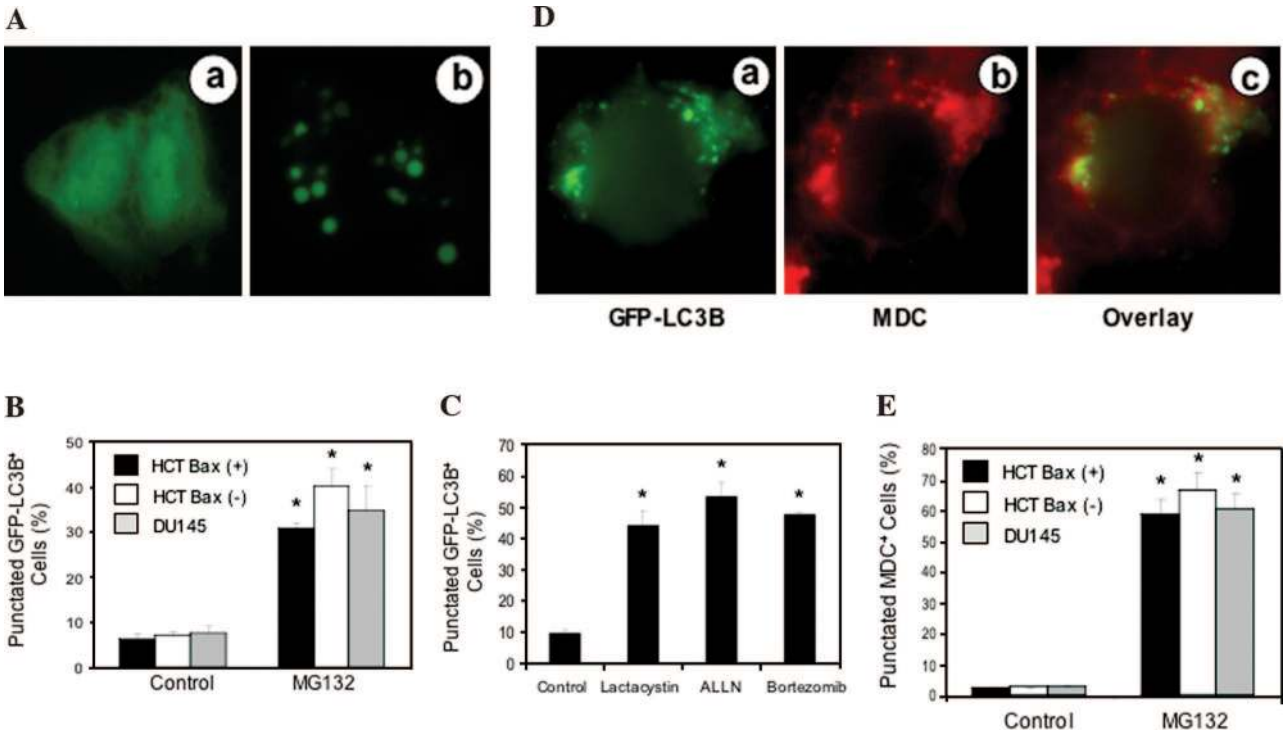

Figure 2. Membrane translocation of GFP-LC3B in response to proteasome inhibition. **A:** DU145 cells were transfected with GFP-LC3B, treated with vehicle control (**a**) or MG132 (5 μmol/L, **b**) for 24 hours and then examined by fluorescence microscopy. **B:** Quantification of punctated GFP-LC3B-positive HCT 116 (black column), Bax-deficient HCT 116 (white column), and DU145 (gray column) cells following the treatment with MG132 (mean ± SD). **C:** HCT116-Bax-deficient cells stably expressing GFP-LC3B were treated with vehicle control, lactacystin (5 μmol/L), ALLN (10 μmol/L), or bortezomib (20 nmol/L) for 24 hours. Percentages of cells with punctated GFP-LC3B signals were determined (mean ± SD). **D:** Bax-positive HCT 116 cells were transfected with GFP-LC3B, treated with MG132 (1 μmol/L) for 24 hours, and then stained with MDC (200 μmol/L), followed by fluorescence microscopy. **E:** Quantification of punctated MDC-positive cells in Bax-positive HCT 116 (black column), Bax-deficient HCT 116 (white column), and DU145 (gray column) cells treated with MG132. $^*P < 0.01$ by Z-test between the control and the treated groups.

degree of stress. It is possible that autophagy induced by the inhibition of proteasome function might serve as a compensatory mechanism in response to protein accumulation to alleviate the toxicity of proteasome inhibitors. Indeed, we found that there was a noticeable increase in the polyubiquitinated proteins in HCT 116 cells when the expression of Atg6 or Atg8/LC3B was suppressed by specific siRNA (Figure 5A). MG132 induced a much more significant elevation of the polyubiquitinated proteins, as would be predicted. However, simultaneous use of the siRNA against Atg6 or Atg8/LC3B and MG132 resulted in the most abundant accumulation of the polyubiquitinated proteins (Figure 5A). The ubiquitinated proteins were present mainly in the nuclei in a dispersed way in the untreated HCT 116 cells but formed perinuclear aggregates following MG132 treatment (Figure 5B). Inhibition of autophagy did not induce aggregate formation by itself (data not shown) but exacerbated it in MG132-treated cells (Figure 5, B and C). These findings indicated that autophagy could participate in the clearance of polyubiquitinated proteins and ubiquitinated protein aggregates in these cells, particularly when the proteasome functions were inhibited. Indeed, confocal microscopic analysis indicated that the GFP-LC3B puncta, which would represent the autophagic vacuoles, were colocalized with the ubiquitinated aggregates (Figure 5D).

Retrotranslocation of misfolded proteins from the ER and their cytoplasmic polyubiquitination and degradation are tightly coupled processes,[2] and it has been noted that proteasome inhibition leads to ER stress.[19,20] Given the evidence for collaboration between autophagy and the UPS in degrading misfolded proteins, we investigated whether suppression of autophagy could exacerbate ER stress caused by proteasome inhibition. We noted that proteasome inhibitors could elicit a significant degree of cellular vacuolization (Figure 6, A–C). These vacuoles did not seem to represent the ongoing process of autophagy but rather the consequences of ongoing ER stress. Both immunostaining with an anti-calnexin antibody and electron microscopic analysis indicated that the vacuoles consisted of dilated and expanded ER lumens (Figure 6, D and E), which most likely indicated ER stress.[3,21] Furthermore, there was a significant increase of proteins involved in the UPR, such as BiP, ATF4, and CHOP, in the treated cells in response to ER stress (Figure 6F).

Cellular vacuolization/ER stress seemed to be upstream of the death execution programs, as it occurred in both Bax-positive and Bax-negative HCT 116 cells and was not inhibited by z-Vad-fmk (Figure 6A). In contrast, suppression of autophagy using either 3-MA or specific siRNA against *Atg5*, *Atg6/Beclin1*, *Atg7*, or *Atg8/LC3B* in either HCT 116 or DU145 cells all led to an enhancement of proteasome inhibitor-induced cellular vacuolization and ER dilation as observed by either light microscopy or electron microscopy (Figure 6, B, C, and G). Finally, the ER stress-initiated caspase-4 activation[20,22] was also sig-

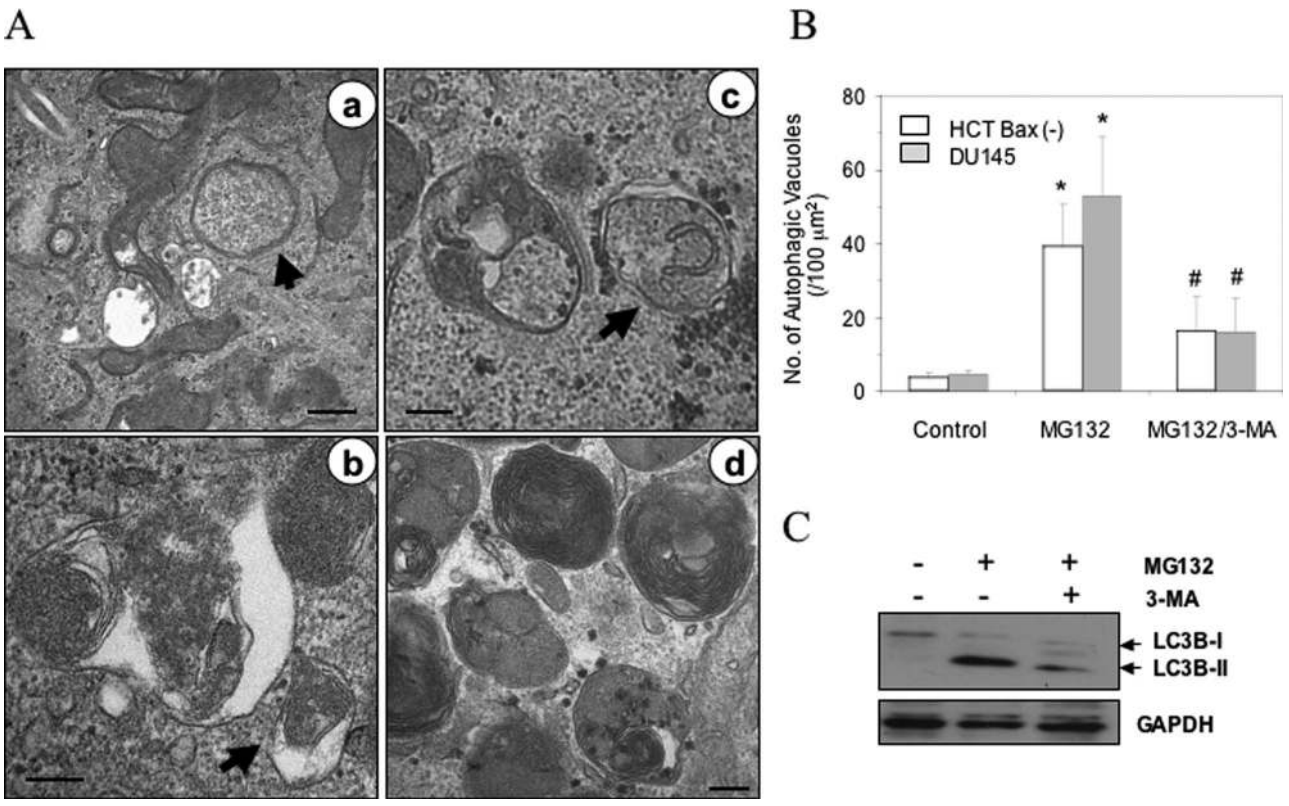

Figure 3. Electron microscopic detection of autophagic vacuoles in proteasome inhibitor-treated cells. **A:** Electron micrographs of HCT 116 cells (**a** and **b**) and DU145 cells (**c** and **d**) treated with MG132 (0.1 to 0.5 μmol/L) for 16 hours. Note the double membrane (**a**, **arrow**) or the multimembrane (**d**) structure of the AVs. **Arrows** also indicate AVs with the contents of cytosol (**a**), mitochondria (**b**), or ER (**c**). Scale bars: 0.5 μm (**a**), 0.2 μm (**b**), 0.25 μm (**c**), and 0.1 μm (**d**). **B:** The number of AVs per 100 μm^2 of cytoplasm area (means ± SD) was quantified in Bax-deficient HCT 116 (white column) and DU145 (gray column) cells treated with MG132 (0.1 and 0.25 μmol/L, respectively) in the presence or absence of 3-MA (10 mmol/L). * and $^{\#}P < 0.01$ (*MG132-treated group versus the control; $^{\#}$MG132 plus 3-MA versus MG132 alone) by one-way analysis of variance. **C:** Bax-deficient HCT 116 cells were treated with MG132 (0.5 μmol/L) plus or minus 3-MA (10 mmol/L), and the processing of LC3B was examined by immunoblot analysis.

nificantly increased when both proteasome function and autophagy were inhibited (Figure 6H), consistent with the increased cell death (Figure 4). Taken together, our study indicates that autophagy serves to reduce polyubiquitination protein accumulation and alleviate ER stress, thus inhibiting cell death caused by ER decompensation.

IRE1 Promoted Autophagy on Proteasome Inhibition

The close relationship of proteasome inhibition, ER stress, and autophagy suggest that proteasome inhibitors could induce autophagy via ER stress. Chemicals that directly induced ER stress, such as tunicamycin (TM), A23187, and thapsigargin (TG) have been shown to induce autophagy in both mammalian cells and in yeast.[21,23–26] We therefore examined whether the major ER stress remedy pathway, the UPR, could be involved in the autophagy induced by proteasome inhibitors. There are three major UPR pathways mediated by ATF6, PERK, and IRE1. The IRE1 pathway perhaps deserves the most attention, since it is also conserved in the yeast and has been shown to be involved in autophagy induced by directly stressing ER.[25] We thus examined whether IRE1 was required for proteasome inhibitor-induced autophagy.

Wild-type and IRE1α/β-deficient MEFs were treated with bortezomib or MG132, and induction of autophagy was monitored by immunoblot analysis of LC3B-II and by GFP-LC3B punctation. Deletion of IRE1α/β significantly inhibited these responses following proteasome inhibition (Figure 7, A–C). Consistent with previous work, autophagy induced by the classic ER stress inducers (A23187, TM, or TG) was also dependent on IRE1α/β (Figure 7, A–C). This observation was furthermore confirmed in HCT 116 cells via the siRNA-mediated knockdown of IRE1α expression (Figure 7, D and E).

These observations implicate IRE1 in proteasome inhibitor-induced autophagy. In mammalian cells, two well-defined mechanisms are activated by IRE1. First, the transcript of *XBP-1* gene undergoes an alternative splicing, resulting in an active transcription factor that participates in UPR.[27,28] Second, JNK can be activated to participate in cell death.[29,30] We thus examined the role of JNK and XBP-1 in proteasome inhibitor-induced autophagy.

Activation of JNK by proteasome inhibitors has been well documented,[31] and we found that this activation was largely dependent on IRE1 (Figure 8A). A specific JNK inhibitor, SP600125, caused a significant reduction of GFP-LC3B puncta in bortezomib-treated MEFs (Figure 8,

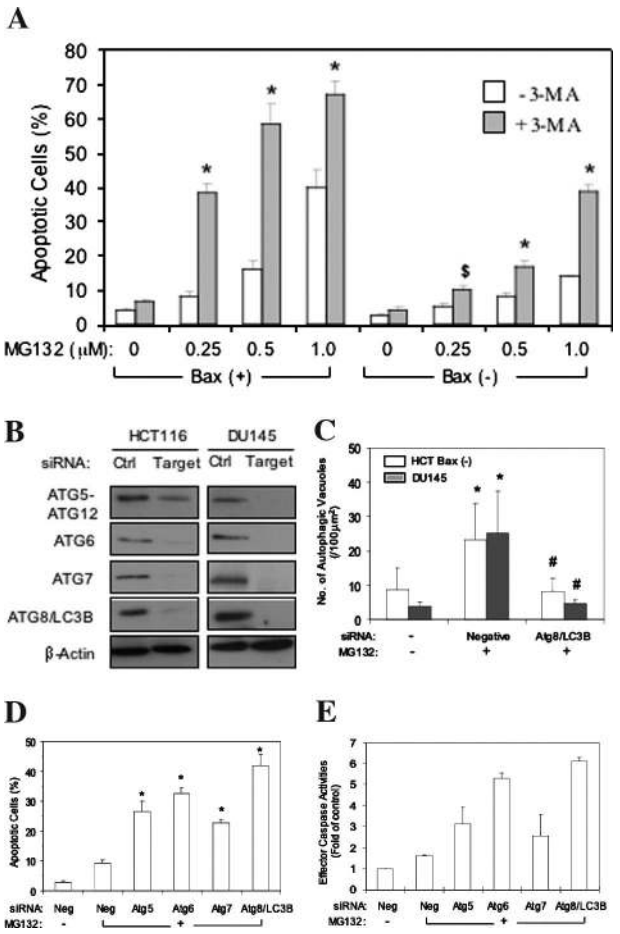

Figure 4. Suppression of autophagy enhances proteasome inhibitor-induced cell death in cancer cells. **A:** Bax-positive and Bax-deficient HCT 116 cells were treated with MG132 in the presence (closed column) or absence (open column) of 3-MA (10 mmol/L) for 24 hours and then stained with Hoechst 33328. Cells with apoptotic nuclear features were defined as apoptotic cells. $^{*}P < 0.01$ and $^{\$}P < 0.05$ by Z-test between groups without 3-MA and groups with 3-MA for each MG132 dosage and cell line. **B:** Bax-deficient HCT 116 and DU145 cells were transfected with indicated siRNA against specific Atg genes (target) or a negative control siRNA (Ctrl) for 48 hours followed by immunoblot with different antibodies. Atg5 was detected as the complex with Atg12. **C:** Bax-deficient HCT 116 (white column) and DU145 (gray column) cells were transfected with 120 nmol/L siRNA against Atg8/LC3B or a negative control siRNA for 36 hours before being treated with MG132. The number of AVs per 100 μm^2 of cytoplasm area (means ± SD) was then quantified. * and $^{\#}P < 0.01$ by one-way analysis of variance for both cell lines (*MG132 plus negative siRNA versus the control; $^{\#}$MG132 plus siRNA-LC3B versus MG132 plus negative siRNA). **D** and **E:** Bax-deficient HCT 116 cells were transfected with specific siRNA or a negative control (Neg) as indicated and treated with MG132 (0.25 μmol/L) for 16 hours. Apoptotic cells (**D**) were determined as in **A**. $^{*}P < 0.01$ by Z-test (MG132 plus specific siRNA versus MG132 plus negative siRNA). Effector caspase activities (**E**) were measured using DEVD-AFC as the substrate, and the results were expressed as the fold increase over the nontreated control group.

B and C) and HCT 116 cells (Figure 8D). Similar effects were observed for A23187-treated cells (Figure 8, B and C). On the other hand, we found that proteasome inhibitors could not induce XBP-1 alternative splicing (data not shown), consistent with an earlier study.[32] Furthermore, deletion of XBP-1 did not affect the punctation of GFP-LC3B (Figure 8, C and D) or LC3B-II formation (Figure 8E) induced by these agents, suggesting that XBP-1 could be dispensed. Interestingly, based on these criteria, XBP-1 seemed to be equally nonessential for autophagy induced by A23187, TG, or TM (Figure 8, B, C, and E), despite the fact that they could induce alternative splicing of *XBP-1* (data not shown).[27,28] No further suppression in GFP-LC3B puncta was observed when SP600125 was used in *XBP-1*-deficient cells treated with the same agents (Figure 8, B and C). Taken together, these results indicate that JNK, but not XBP-1, could participate in proteasome inhibitor-induced autophagy downstream of IRE1.

Discussion

The Ubiquitin Proteasome System and Autophagy Are Functionally Linked

Although both UPS and autophagy serve to degrade intracellular contents, the two systems are generally thought to be independent from each other in terms of the degradation mechanisms, the types of contents to be degraded, the signals activating the pathway, and the physiological significance of the degradation.[1,6,7] We here show that inhibition of UPS can activate autophagy. Simultaneous inhibition of autophagy promotes accumulations of ubiquitinated protein aggregates, ER stress, and cell death. Whereas the evidence presented here that UPS and autophagy are functionally linked is derived from inhibiting proteasome function, evidence indicating such a connection has also emerged in other studies where autophagy machinery is disrupted. Mice deficient in the key autophagy genes, *atg5* or *atg7*, accumulate ubiquitinated protein aggregates in the neurons at an early age and develop symptoms similar to those of human neurodegenerative diseases.[33,34]

Misfolded protein aggregates, which are often polyubiquitinated, can contribute to the pathogenesis of many human diseases.[35] Notably, proteasome functions are often impaired in these cases and are likely not able to degrade the aggregate fully.[36–38] Autophagic vacuoles were frequently found in these cases[36,39,40] and, indeed, autophagy has been shown to be able to participate in the removal of misfolded/unfolded proteins or protein aggregates.[23,41–45]

Taken together, these studies indicate that autophagy can participate in the clearance of intracellular contents that were previously thought to be targeted exclusively by the UPS. Autophagy could be activated and play a compensatory role when proteasome function is suppressed.

The Mechanism of Autophagy Activation by Proteasome Inhibitors

We have investigated the molecular mechanisms by which autophagy is activated by the inhibition of proteasome. Because the proteasome inhibitor could induce ER stress, and autophagy serves to relieve ER stress (Figure 6), it is likely that ER stress could constitute a major signal that activates autophagy. Misfolded proteins are known

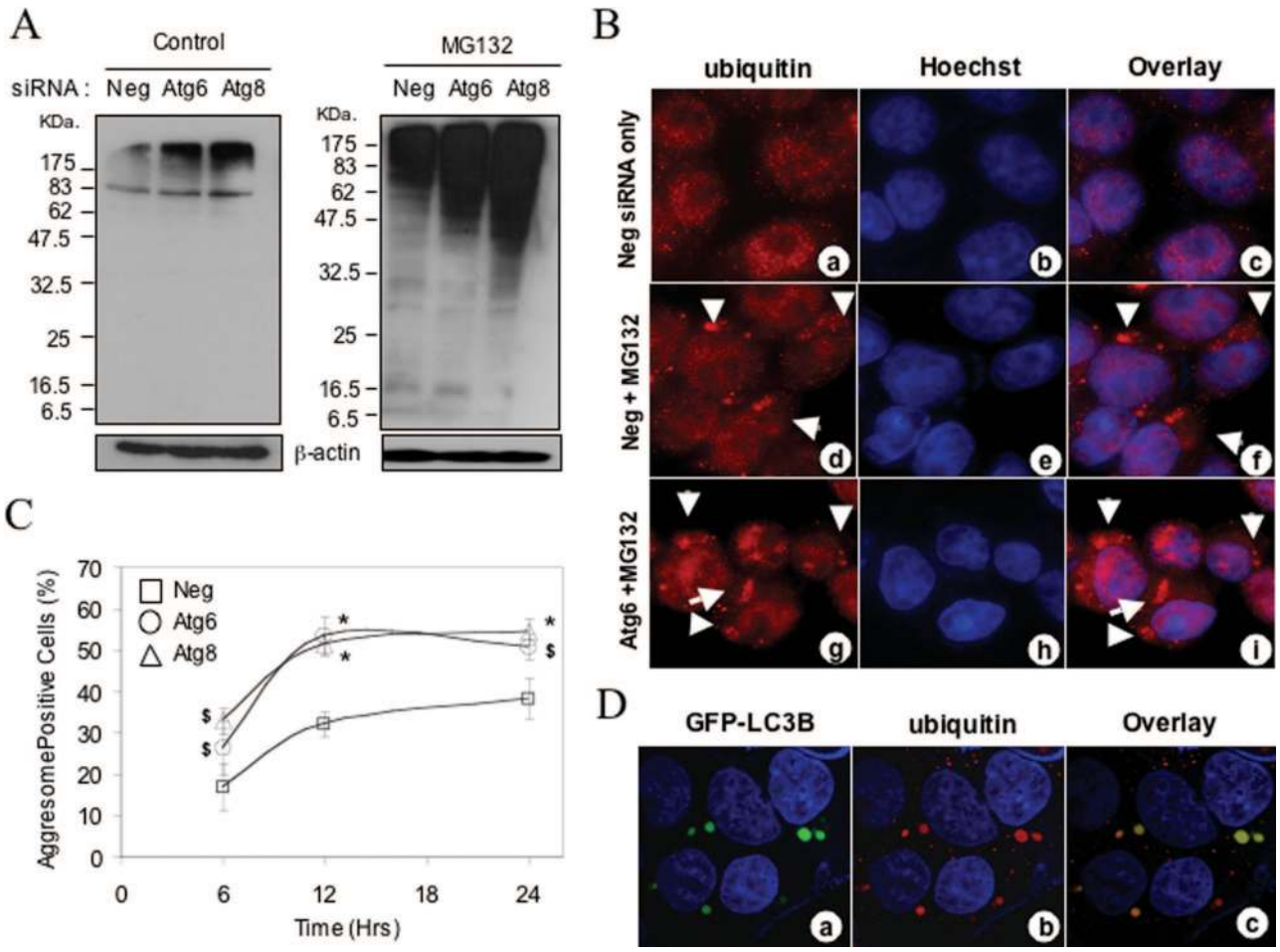

Figure 5. Suppression of autophagy enhances accumulation of ubiquitinated proteins and aggregates in cancer cells. **A:** Bax-deficient HCT 116 cells were transfected with negative siRNA (Neg) or siRNA against Atg8/LC3B or Atg6 for 48 hours and then treated with MG132 (0.5 μmol/L) or with control vehicles for 24 hours. Lysates were prepared in radioimmunoprecipitation assay buffer and separated on sodium dodecyl sulfate-polyacrylamide gel electrophoresis. Immunoblot assay was conducted with the anti-ubiquitin (top panels) and anti-β-actin (bottom panels) antibodies. **B** and **C:** HCT 116 Bax-deficient cells were transfected with designated siRNA and treated with MG132 (0.5 μmol/L) for 24 hours (**B**) or as indicated (**C**). Cells were then fixed with 4% paraformaldehyde and stained with the anti-ubiquitin antibody and the DNA dye Hoechst 33342. Dispersed ubiquitinated proteins could be detected in the nucleus of nontreated cells, but the perinuclear ubiquitinated protein aggregates could be only detected in MG132-treated cells (**arrows**). The latter (aggresome-positive cells) were quantified and expressed as the percentage of total anti-ubiquitin-positive cells (**C**). $^{*}P < 0.01$ and $^{\$}P < 0.05$ by Z-test (specific siRNA versus negative siRNA). **D:** DU145 cells stably expressing GFP-LC3B were treated with bortezomib (10 nmol/L) for 24 hours and then immunostained with an anti-ubiquitin antibody as well as Hoechst 33342 as above. Cells were then subjected to confocal microscopy. **a** shows the GFP-LC3B puncta, whereas **b** shows the ubiquitin-positive aggresomes. Merged image in **c** indicates the colocalization of GFP-LC3B puncta and the aggresomes.

to induce ER stress, whether they are located in the ER lumen or not,[3,4,35,40,46] and as mentioned above, they can induce autophagy. In addition, classic ER stress inducers, such as A23187, thapsigargin, and tunicamycin, can all induce autophagy in mammalian cells[23,25,26] and in yeast.[21,24] The UPR is activated by ER stress and is mediated by the ATF6, PERK, and IRE1 pathways.[3,4] It has been reported that ATF6 is not required for ER stress-induced autophagy.[25] But the PERK-eIF2α pathway is important for autophagy induced by the misfolded pathogenic polyglutamine repeats,[23] and the IRE1-JNK pathway is important for autophagy induced by tunicamycin and thapsigargin.[25] We have found that mutations that compromise signaling in the PERK and eIF2α pathway do not affect the induction of autophagy by proteasome inhibition (data not shown). However, we do find that IRE1 plays an important role (Figure 6). This finding supports the notion that proteasome inhibitors activate autophagy via ER stress. The reason for the differential use of the PERK versus IRE1 pathway in autophagy induced by different agents is currently not clear despite the fact that they all can induce ER stress.

IRE1-mediated UPR is conserved in the yeast, in which ER stress could also induce autophagy.[21,24] IRE1 can activate a transcription factor, XBP-1, via its endoribonuclease activity,[27,28] and a stress kinase, JNK, via its association with TRAF2[29] and activation of a MAP3K, ASK-1.[30] We have found that markers of autophagy were activated to wild-type levels in XBP-1 knockout MEFs exposed to proteasome inhibitors A23187, TG, or TM. On the other hand, we find that JNK can participate in proteasome inhibitor-induced autophagy. JNK has also been found important in autophagy induced by the ER stress inducers A23187 (Figure 8) and TG.[25] These findings affirm the notion that proteasome inhibitors could induce autophagy via ER stress. Although in this setting JNK but not XBP-1 seems to be important for

autophagy induction downstream of IRE1 signaling, our studies do not exclude the possibility that XBP-1 can participate in autophagy induced through other means and do not exclude simultaneous participation of other mechanisms in parallel with the JNK signaling, in particular the calcium/calmodulin-dependent kinase kinase-β pathway that is also active in ionomycin and TG-induced autophagy.[47] Although it is currently unclear how JNK promotes autophagy, it is tempting to speculate that it may act on the mammalian target of rapamycin pathway as well, which seems to be central to the control of autophagy in many instances.[6–8]

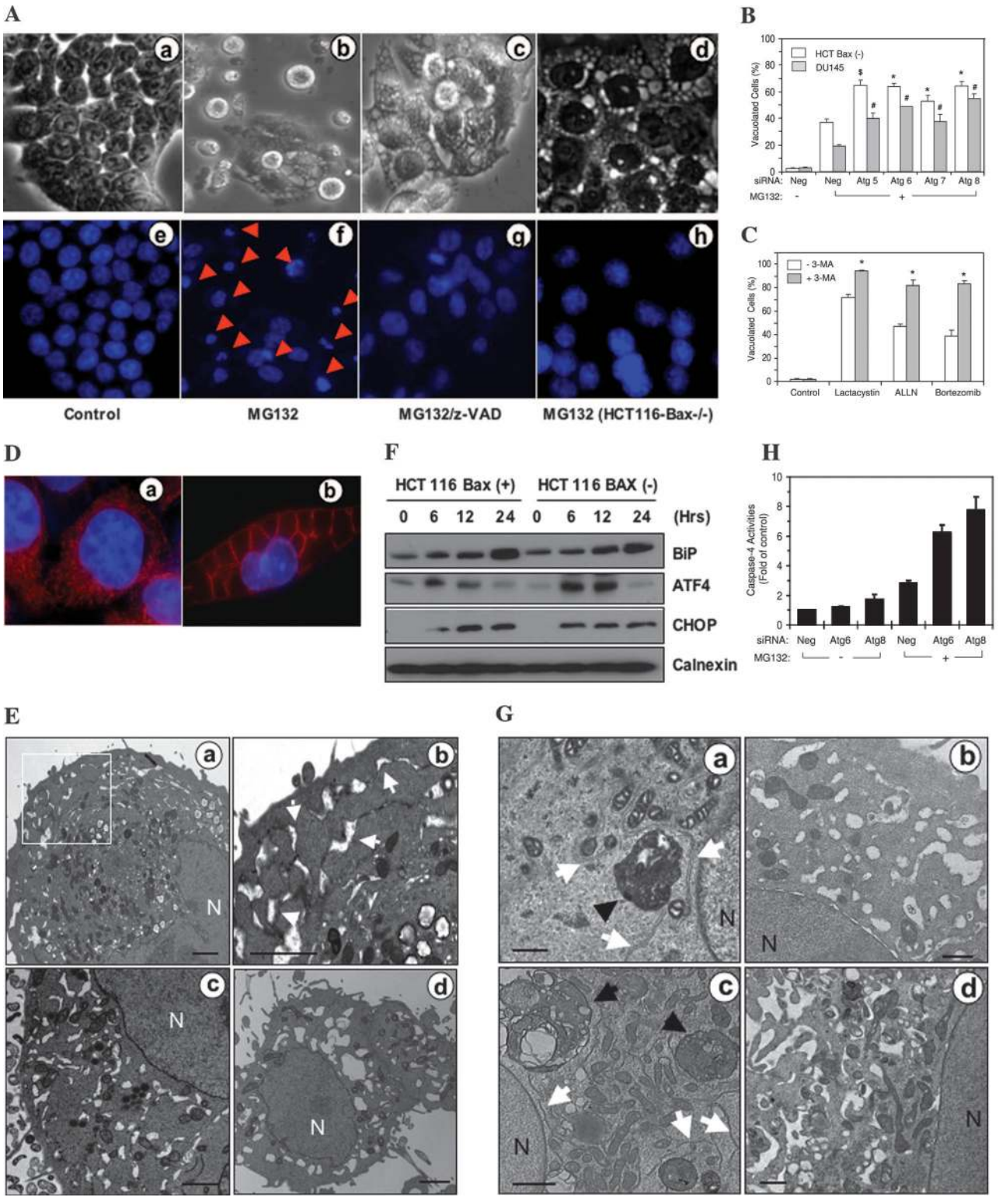

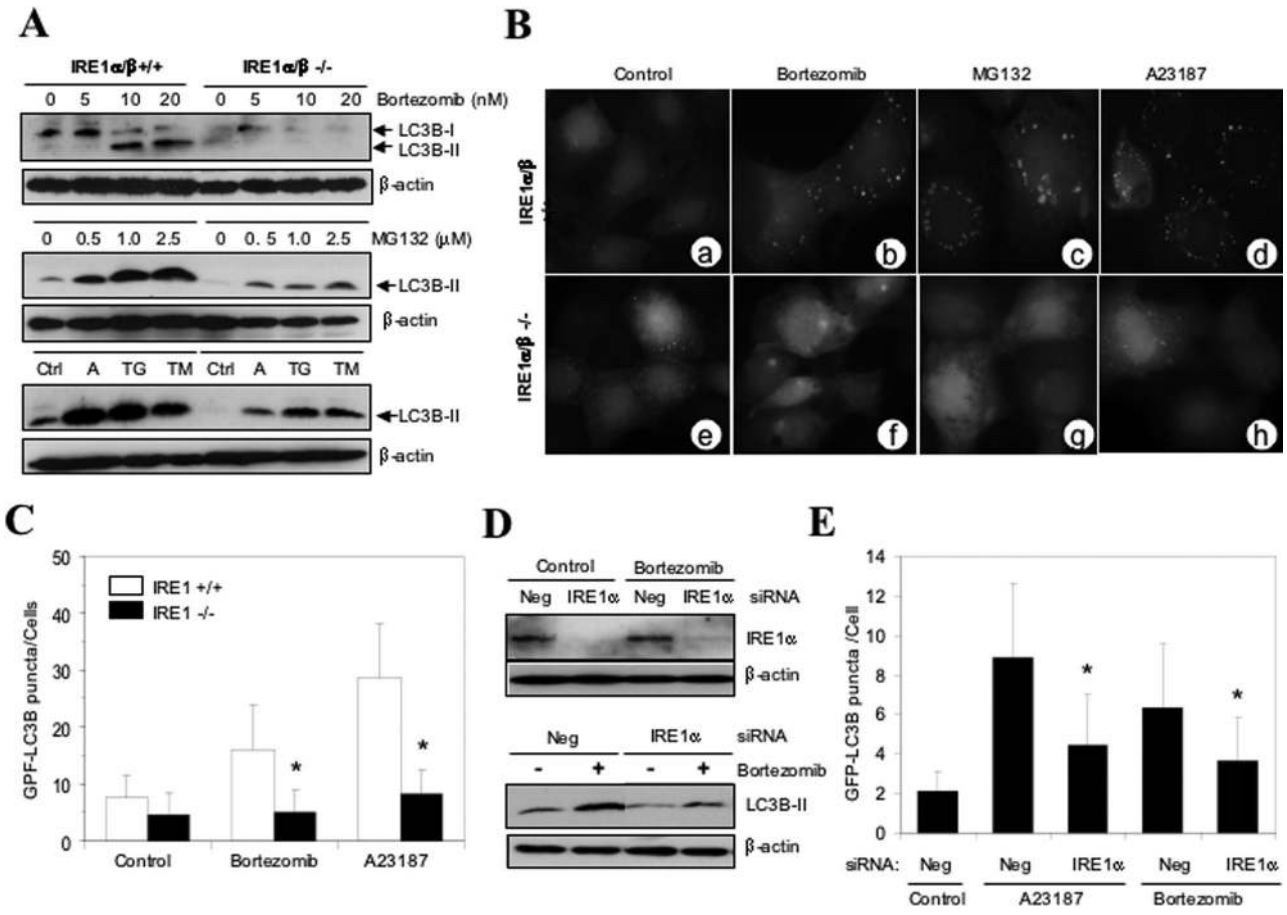

Figure 7. IRE1 is critically involved in proteasome inhibitor-induced autophagy. **A:** Wild-type and IRE1α/β-deficient MEFs were treated with bortezomib or MG132 at the designated concentrations or with the ER stress inducers A23187 (A, 2.5 μmol/L), thapsigargin (TG, 0.5 μmol/L), or tunicamycin (TM, 5 μg/ml) for 24 hours. Immunoblot assays were then conducted. **B** and **C:** Wild-type and IRE1α/β-deficient MEFs expressing GFP-LC3B were treated with vehicle control, bortezomib (10 nmol/L), MG132 (1 μmol/L), or A23187 (2.5 μmol/L) for 24 hours. The punctation of GFP-LC3B was assessed (**B**). The number of puncta per cell (mean ± SD) was quantified (**C**). $^{*}P < 0.01$ by one-way analysis of variance (IRE1α/β-deficient MEFs versus IRE1α/β-positive MEFs). **D** and **E:** HCT 116 Bax-deficient cells were transfected with a specific siRNA against IRE1α or a negative control (Neg) siRNA for 24 to 48 hours. They were treated with bortezomib (10 nmol/L) or A23187 (2.5 μmol/L) for an additional 18 to 24 hours. Immunoblot assays were then conducted (**D**). Alternatively, the extent of GFP-LC3B punctation was quantified (**E**). $^{*}P < 0.01$ by one-way analysis of variance (siRNA-IRE1α versus negative siRNA for A23187 and bortezomib-treated groups).

Autophagy Functions to Alleviate ER Stress and Therefore Diminishes the Death Signal Strength to Suppress Cell Death

Proteasome inhibitors can induce apoptotic cell death, particularly in Bax-positive cells (Figure 4). Interestingly, suppressing autophagy enhances the apoptotic death not only in the Bax-positive HCT 116 cells but also in an appreciable number of Bax-deficient cells. One attractive explanation is that under permissive conditions, autophagy induced by proteasome inhibition helps to reduce death stimulation to the level that it will only activate the

Figure 6. Suppression of autophagy enhances proteasome inhibitor-induced ER stress in cancer cells. **A:** Bax-positive (**a–c**, **e–g**) and Bax-deficient (**d** and **h**) HCT 116 cells were treated with MG132 (1 μmol/L) in the presence or absence of z-VAD (50 μmol/L) as indicated and analyzed 24 hours later by phase microscopy (**a–d**) and Hoechst staining (**e–h**). **Arrows** indicate the apoptotic cells (**f**), which were greatly reduced in the presence of z-VAD (**g**) or in the absence of Bax (**h**). Note that cellular vacuolization was not affected by z-VAD or Bax. **B:** Bax-deficient HCT 116 or DU145 cells were transfected with siRNA against the indicated *Atg* genes or a negative control siRNA (Neg) for 48 hours before they were treated with MG132 (0.25 or 0.5 μmol/L, respectively). Percentage of vacuolated cells was quantified 24 hours later. * and $^{\#}P < 0.01$; $^{\$}P < 0.05$ by Z-test (MG132 plus specific siRNA versus MG132 plus negative siRNA in each cell line. * and $^{\$}$HCT 116 cells; $^{\#}$DU145 cells). **C:** HCT 116 Bax-negative cells were treated with lactacystin (5 μmol/L), ALLN (10 μmol/L), or bortezomib (20 nmol/L) for 24 hours in the presence (closed column) or absence (open column) of 3-MA (10 mmol/L). Percentage of cells with vacuoles was determined. $^{*}P < 0.01$ by Z-test (groups without 3-MA versus groups with 3-MA for each proteasome inhibitor). **D:** Bax-deficient HCT 116 cells were treated with vehicle control (**a**) or MG132 (1 μmol/L **b**) for 24 hours followed by immunostaining with an anti-calnexin antibody. **E:** DU145 (**a** and **b**) or Bax-deficient HCT 116 cells (**c** and **d**) were treated with MG132 (1 or 5 μmol/L, respectively) for 24 hours and then analyzed by electron microscopy. Representative images are shown to indicate the progressive dilation of the ER lumen. The boxed area in **a** is enlarged in **b**. **Arrows** indicate the dilated segment of selected ER (**b**). Scale bars: 0.25 μm (**a** and **b**), 2 μm (**c** and **d**). N, nucleus. **F:** HCT 116 cells were treated with MG132 (1 μmol/L) for indicated times followed by immunoblot analysis. **G:** Bax-deficient HCT 116 (**a** and **b**) and DU145 (**c** and **d**) cells were transfected with siRNA against *Atg8/LC3B* (**b** and **d**) or a negative siRNA (**a** and **c**) for 36 hours before they were treated with MG132 (0.1 or 0.25 μmol/L, respectively) for 16 hours. Representative electron micrographs are shown to indicate the suppression of autophagy and the enhancement of ER dilation in Atg8/LC3B-knocked-down cells (**b** and **d**). N, nucleus; **black arrows**, autophagic vacuoles; **white arrows**, nondilated ER. Scale bar = 1 μm. **H:** Bax-deficient HCT 116 cells were transfected with the indicated siRNA and treated with MG132 as in **F**. Total cell lysates were prepared, and caspase-4 activity was measured using Ac-LEVD-AFC as the substrate. The results were expressed as the fold of increase over the nontreated control group.

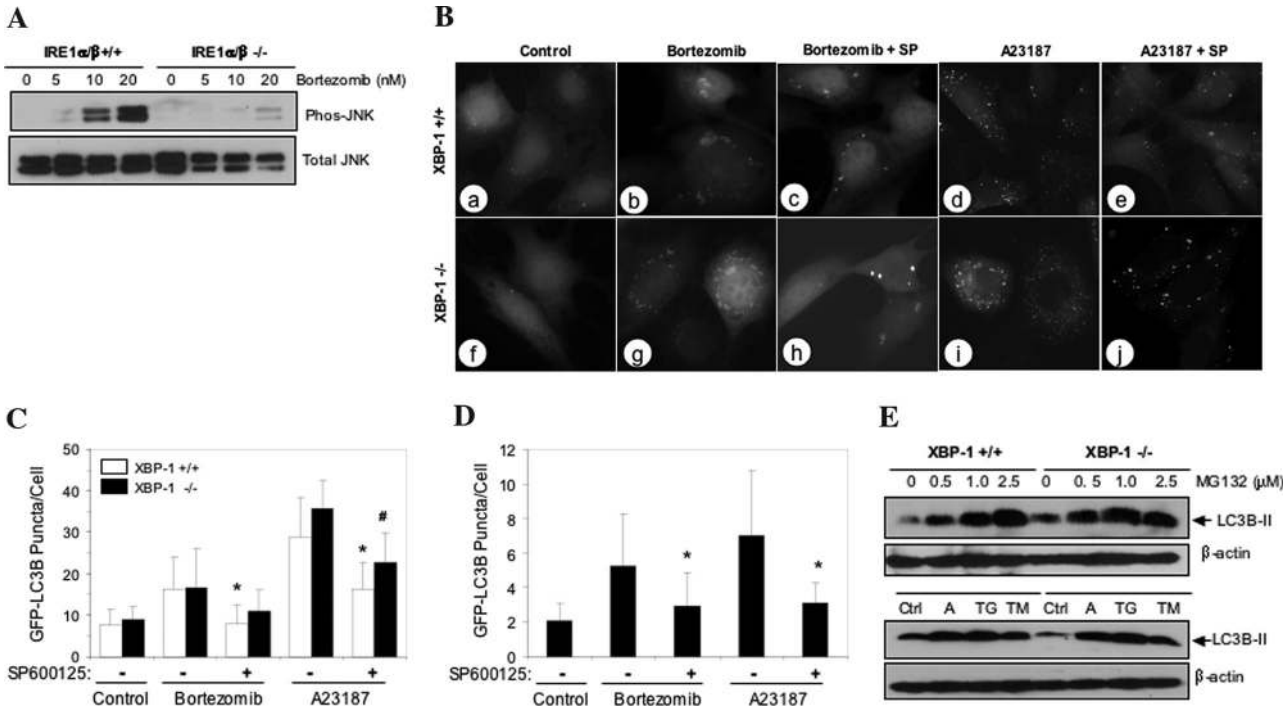

Figure 8. JNK but not XBP-1 contributes to proteasome inhibitor-induced autophagy. **A:** Wild-type and IRE1α/β-deficient MEFs were stimulated with bortezomib at the designated concentrations for 24 hours. Cells were harvested, and immunoblot assay was conducted for total JNK and phosphorylated JNK. **B** and **C:** Wild-type (**a–e**) and *XBP-1*-deficient (**f–j**) MEFs were treated with bortezomib (20 nmol/L, **b**, **c**, **g**, and **h**) or A23187 (2.5 μmol/L, **d**, **e**, **i**, and **j**) in the presence (**c**, **e**, **h**, and **j**) or absence (**b**, **d**, **g**, and **i**) of JNK inhibitor, SP600126 (25 μmol/L) for 16 hours. The punctation pattern of GFP-LC3B was assessed (**B**) and quantified (**C**). * and $^{\#}P < 0.01$ by one-way analysis of variance (SP600125 versus vehicle control for bortezomib or A23187-treated groups. *XBP-$1^{+/+}$ cells; $^{\#}$XBP-$1^{-/-}$ cells). **D:** Bax-deficient HCT 116 cells that stably expressing GFP-LC3B were treated with vehicle control, bortezomib (20 nmol/L), or A23187 (2.5 μmol/L) with or without SP600126 (25 μmol/L) for 16 hours. The punctation pattern of GFP-LC3B was assessed and quantified. $^{*}P < 0.01$ by one-way analysis of variance (SP600125 versus vehicle control for bortezomib or A23187-treated groups). **E:** Wild-type and *XBP-1*-deficient MEFs were treated with MG132 at the designated concentrations or with the ER stress inducers A23187 (A, 2.5 μmol/L), thapsigargin (TG, 0.5 μmol/L), or tunicamycin (TM, 5 μg/ml) for 24 hours. Immunoblot assay was then conducted.

more sensitive pro-death molecule Bax but not the less sensitive pro-death molecule Bak, which is expressed in the Bax-deficient HCT 116.[14,48] A previous study had shown that apoptosis could be induced in Bax-deficient but Bak-positive HCT 116 cells with stronger death stimulations.[48] In addition, even in the Bax-positive cells, apoptosis may be suppressed by autophagy. Suppression of autophagy could thus lead to a stronger death signal in the cells. This notion is supported by other studies where autophagy is protective against cell death[7,49,50] and the toxicity of misfolded proteins, such as the pathogenic polyglutamine repeats.[23,41]

This notion of autophagy being able to reduce death signal strength suggests that autophagy may exert the protection at an upstream step. Proteasome inhibitors can induce cell death via multiple mechanisms,[32] including the induction of ER stress, which is particularly relevant to the current study.[19,20] Inhibition of proteasome function leads to the accumulation of polyubiquitinated proteins and likely causes the accumulation of misfolded proteins in the ER due to the blockage of ER-associated degradation. These events could cause ER stress and cell death. It seems that autophagy activated in this scenario aims to compensate for the reduced proteasome function so that proteins that fail to be degraded by the UPS could be cleared up via autophagy (Figure 5). By doing so, autophagy ameliorates ER stress and suppresses proteasome inhibitor-induced death at an upstream site of the death pathway (Figures 4 and 6). In this role, autophagy is protective against ER stress and ER decompensation. In summary, the functional coupling of autophagy to UPS provides a compensatory mechanism for degrading misfolded proteins and reducing cell death during proteasome inhibition, in which ER stress is critical for autophagy induction and is in turn mitigated by autophagy.

Acknowledgments

We are indebted to Dr. Noboru Mizushima (The Tokyo Metropolitan Institute of Medical Science, Tokyo, Japan) for anti-Atg5 antibody, Dr. Bert Vogelstein (The Johns Hopkins University, Baltimore, MD) for HCT 116 cell lines, and Dr. Laurie H. Glimcher (Harvard University School of Public Health, Boston, MA) for XBP-1-deficient cells. We also thank Marc Rubin, Ana Lopez, and Mara Sullivan for expert technical assistance in electron microscopy.

References

1. Hershko A, Ciechanover A: The ubiquitin system. Annu Rev Biochem 1998, 67:425–479

2. Meusser B, Hirsch C, Jarosch E, Sommer T: ERAD: the long road to destruction. Nat Cell Biol 2005, 7:766–772
3. Schroder M, Kaufman RJ: The mammalian unfolded protein response. Annu Rev Biochem 2005, 74:739–789
4. Harding HP, Calfon M, Urano F, Novoa I, Ron D: Transcriptional and translational control in the mammalian unfolded protein response. Annu Rev Cell Dev Biol 2002, 18:575–599
5. Rao RV, Ellerby HM, Bredesen DE: Coupling endoplasmic reticulum stress to the cell death program. Cell Death Differ 2004, 11:372–380
6. Levine B, Klionsky DJ: Development by self-digestion: molecular mechanisms and biological functions of autophagy. Dev Cell 2004, 6:463–477
7. Lum JJ, DeBerardinis RJ, Thompson CB: Autophagy in metazoans: cell survival in the land of plenty. Nat Rev Mol Cell Biol 2005, 6:439–448
8. Kamada Y, Sekito T, Ohsumi Y: Autophagy in yeast: a TOR-mediated response to nutrient starvation. Curr Top Microbiol Immunol 2004, 279:73–84
9. Kirkegaard K, Taylor MP, Jackson WT: Cellular autophagy: surrender, avoidance and subversion by microorganisms. Nat Rev Microbiol 2004, 2:301–314
10. Shintani T, Klionsky DJ: Autophagy in health and disease: a double-edged sword. Science 2004, 306:990–995
11. Klionsky DJ, Cregg JM, Dunn WA, Emr SD, Sakai Y, Sandoval IV, Sibirny A, Subramani S, Thumm M, Veenhuis M, Ohsumi Y: A unified nomenclature for yeast autophagy-related genes. Dev Cell 2003, 5:539–545
12. Kabeya Y, Mizushima N, Ueno T, Yamamoto A, Kirisako T, Noda T, Kominami E, Ohsumi Y, Yoshimori T: LC3, a mammalian homologue of yeast Apg8p, is localized in autophagosome membranes after processing. EMBO J 2000, 19:5720–5728
13. Kuma A, Hatano M, Matsui M, Yamamoto A, Nakaya H, Yoshimori T, Ohsumi Y, Tokuhisa T, Mizushima N: The role of autophagy during the early neonatal starvation period. Nature 2004, 432:1032–1036
14. Zhang L, Yu J, Park BH, Kinzler KW, Vogelstein B: Role of BAX in the apoptotic response to anticancer agents. Science 2000, 290:989–992
15. Ding WX, Ni HM, DiFrancesca D, Stolz DB, Yin XM: Bid-dependent generation of oxygen radicals promotes death receptor activation-induced apoptosis in murine hepatocytes. Hepatology 2004, 40:403–413
16. Biederbick A, Kern HF, Elsasser HP: Monodansylcadaverine (MDC) is a specific in vivo marker for autophagic vacuoles. Eur J Cell Biol 1995, 66:3–14
17. Fengsrud M, Sneve ML, Overbye A, Seglen PO: Structural aspects of mammalian autophagy. Autophagy, chapter 2. Edited by DJ Klionsky. Georgetown, TX, Landes Bioscience, 2004, pp 11–25
18. Seglen PO, Gordon PB: 3-Methyladenine: specific inhibitor of autophagic/lysosomal protein degradation in isolated rat hepatocytes. Proc Natl Acad Sci USA 1982, 79:1889–1892
19. Fribley A, Zeng Q, Wang CY: Proteasome inhibitor PS-341 induces apoptosis through induction of endoplasmic reticulum stress-reactive oxygen species in head and neck squamous cell carcinoma cells. Mol Cell Biol 2004, 24:9695–9704
20. Nawrocki ST, Carew JS, Dunner K Jr, Boise LH, Chiao PJ, Huang P, Abbruzzese JL, McConkey DJ: Bortezomib inhibits PKR-like endoplasmic reticulum (ER) kinase and induces apoptosis via ER stress in human pancreatic cancer cells. Cancer Res 2005, 65:11510–11519
21. Bernales S, McDonald KL, Walter P: Autophagy counterbalances endoplasmic reticulum expansion during the unfolded protein response. PLoS Biol 2006, 4:e423
22. Hidvegi T, Schmidt BZ, Hale P, Perlmutter DH: Accumulation of mutant α1-antitrypsin Z in the endoplasmic reticulum activates caspases-4 and -12, NFκB, and BAP31 but not the unfolded protein response. J Biol Chem 2005, 280:39002–39015
23. Kouroku Y, Fujita E, Tanida I, Ueno T, Isoai A, Kumagai H, Ogawa S, Kaufman RJ, Kominami E, Momoi T: ER stress (PERK/eIF2α phosphorylation) mediates the polyglutamine-induced LC3 conversion, an essential step for autophagy formation. Cell Death Differ 2007, 14:230–239
24. Yorimitsu T, Nair U, Yang Z, Klionsky DJ: Endoplasmic reticulum stress triggers autophagy. J Biol Chem 2006, 281:30299–30304
25. Ogata M, Hino S, Saito A, Morikawa K, Kondo S, Kanemoto S, Murakami T, Taniguchi M, Tanii I, Yoshinaga K, Shiosaka S, Hammarback JA, Urano F, Imaizumi K: Autophagy is activated for cell survival after endoplasmic reticulum stress. Mol Cell Biol 2006, 26:9220–9231
26. Ding WX, Ni HM, Gao W, Hou YF, Melan MA, Chen X, Stolz DB, Shao ZM, Yin XM: Differential effects of endoplasmic reticulum stress-induced autophagy on cell survival. J Biol Chem 2007, 282:4702–4710
27. Calfon M, Zeng H, Urano F, Till JH, Hubbard SR, Harding HP, Clark SG, Ron D: IRE1 couples endoplasmic reticulum load to secretory capacity by processing the XBP-1 mRNA. Nature 2002, 415:92–96
28. Yoshida H, Matsui T, Yamamoto A, Okada T, Mori K: XBP1 mRNA is induced by ATF6 and spliced by IRE1 in response to ER stress to produce a highly active transcription factor. Cell 2001, 107:881–891
29. Urano F, Wang X, Bertolotti A, Zhang Y, Chung P, Harding HP, Ron D: Coupling of stress in the ER to activation of JNK protein kinases by transmembrane protein kinase IRE1. Science 2000, 287:664–666
30. Nishitoh H, Matsuzawa A, Tobiume K, Saegusa K, Takeda K, Inoue K, Hori S, Kakizuka A, Ichijo H: ASK1 is essential for endoplasmic reticulum stress-induced neuronal cell death triggered by expanded polyglutamine repeats. Genes Dev 2002, 16:1345–1355
31. Adams J: The development of proteasome inhibitors as anticancer drugs. Cancer Cell 2004, 5:417–421
32. Lee AH, Iwakoshi NN, Anderson KC, Glimcher LH: Proteasome inhibitors disrupt the unfolded protein response in myeloma cells. Proc Natl Acad Sci USA 2003, 100:9946–9951
33. Komatsu M, Waguri S, Chiba T, Murata S, Iwata J, Tanida I, Ueno T, Koike M, Uchiyama Y, Kominami E, Tanaka K: Loss of autophagy in the central nervous system causes neurodegeneration in mice. Nature 2006, 441:880–884
34. Hara T, Nakamura K, Matsui M, Yamamoto A, Nakahara Y, Suzuki-Migishima R, Yokoyama M, Mishima K, Saito I, Okano H, Mizushima N: Suppression of basal autophagy in neural cells causes neurodegenerative disease in mice. Nature 2006, 441:885–889
35. Perlmutter DH: The cellular response to aggregated proteins associated with human disease. J Clin Invest 2002, 110:1219–1220
36. Keller JN, Dimayuga E, Chen Q, Thorpe J, Gee J, Ding Q: Autophagy, proteasomes, lipofuscin, and oxidative stress in the aging brain. Int J Biochem Cell Biol 2004, 36:2376–2391
37. Bence NF, Sampat RM, Kopito RR: Impairment of the ubiquitin-proteasome system by protein aggregation. Science 2001, 292:1552-1555
38. Teckman JH, Burrows J, Hidvegi T, Schmidt B, Hale PD, Perlmutter DH: The proteasome participates in degradation of mutant α1-antitrypsin Z in the endoplasmic reticulum of hepatoma-derived hepatocytes. J Biol Chem 2001, 276:44865–44872
39. Ravikumar B, Rubinsztein DC: Can autophagy protect against neurodegeneration caused by aggregate-prone proteins? Neuroreport 2004, 15:2443–2445
40. Teckman JH, Perlmutter DH: Retention of mutant α(1)-antitrypsin Z in endoplasmic reticulum is associated with an autophagic response. Am J Physiol 2000, 279:G961–G974
41. Ravikumar B, Vacher C, Berger Z, Davies JE, Luo S, Oroz LG, Scaravilli F, Easton DF, Duden R, O'Kane CJ, Rubinsztein DC: Inhibition of mTOR induces autophagy and reduces toxicity of polyglutamine expansions in fly and mouse models of Huntington disease. Nat Genet 2004, 36:585–595
42. Kamimoto T, Shoji S, Hidvegi T, Mizushima N, Umebayashi K, Perlmutter DH, Yoshimori T: Intracellular inclusions containing mutant α1-antitrypsin Z are propagated in the absence of autophagic activity. J Biol Chem 2006, 281:4467–4476
43. Shibata M, Lu T, Furuya T, Degterev A, Mizushima N, Yoshimori T, MacDonald M, Yankner B, Yuan J: Regulation of intracellular accumulation of mutant Huntingtin by Beclin 1. J Biol Chem 2006, 281:14474–14485
44. Kruse KB, Brodsky JL, McCracken AA: Characterization of an ERAD gene as VPS30/ATG6 reveals two alternative and functionally distinct protein quality control pathways: one for soluble Z variant of human α-1 proteinase inhibitor (A1PiZ) and another for aggregates of A1PiZ. Mol Biol Cell 2006, 17:203–212
45. Kruse KB, Dear A, Kaltenbrun ER, Crum BE, George PM, Brennan SO, McCracken AA: Mutant fibrinogen cleared from the endoplasmic reticulum via endoplasmic reticulum-associated protein degradation and autophagy: an explanation for liver disease. Am J Pathol 2006, 168:1299–1308; quiz 1404–1295

46. Rao RV, Bredesen DE: Misfolded proteins, endoplasmic reticulum stress and neurodegeneration. Curr Opin Cell Biol 2004, 16:653–662
47. Hoyer-Hansen M, Bastholm L, Szyniarowski P, Campanella M, Szabadkai G, Farkas T, Bianchi K, Fehrenbacher N, Elling F, Rizzuto R, Mathiasen IS, Jäättelä M: Control of macroautophagy by calcium, calmodulin-dependent kinase kinase-β, and Bcl-2. Mol Cell 2007, 25:193–205
48. Chandra D, Choy G, Daniel PT, Tang DG: Bax-dependent regulation of Bak by voltage-dependent anion channel 2. J Biol Chem 2005, 280:19051–19061
49. Degenhardt K, Mathew R, Beaudoin B, Bray K, Anderson D, Chen G, Mukherjee C, Shi Y, Gelinas C, Fan Y, Nelson DA, Jin S, White E: Autophagy promotes tumor cell survival and restricts necrosis, inflammation, and tumorigenesis. Cancer Cell 2006, 10:51–64
50. Boya P, Gonzalez-Polo RA, Casares N, Perfettini JL, Dessen P, Larochette N, Metivier D, Meley D, Souquere S, Yoshimori T, Pierron G, Codogno P, Kroemer G: Inhibition of macroautophagy triggers apoptosis. Mol Cell Biol 2005, 25:1025–1040
51. Ohsumi Y, Mizushima N: Two ubiquitin-like conjugation systems essential for autophagy. Semin Cell Dev Biol 2004, 15:231–236